Inertial effects in the dc+ac driven underdamped Frenkel-Kontorova model: Subharmonic steps, chaos, and hysteresis

J. Tekić,[1] A. E. Botha,[2] P. Mali,[3] and Yu. M. Shukrinov[4,5]

[1] *"Vinca" Institute of Nuclear Sciences, Laboratory for Theoretical and Condensed Matter Physics-020, University of Belgrade, P.O. Box 522, 11001 Belgrade, Serbia*

[2] *Department of Physics, University of South Africa, Science Campus, Private Bag X6, Florida Park 1710, South Africa*

[3] *Department of Physics, Faculty of Science, University of Novi Sad, Trg Dositeja Obradovića 4, 21000 Novi Sad, Serbia*

[4] *BLTP, JINR, Dubna, Moscow Region, 141980, Russian Federation*

[5] *Department of Nanotechnology and New Materials, Dubna State University, Dubna, Moscow Region, 141980, Russian Federation*

(Received 28 November 2018; published 11 February 2019)

The effects of inertial terms on the dynamics of the dc+ac driven Frenkel-Kontorova model were examined. As the mass of particles was varied, the response of the system to the driving forces and appearance of the Shapiro steps were analyzed in detail. Unlike in the overdamped case, the increase of mass led to the appearance of the whole series of subharmonic steps in the staircase of the average velocity as a function of average driving force in any commensurate structure. At certain values of parameters, the subharmonic steps became separated by chaotic windows while the whole structure retained scaling similar to the original staircase. The mass of the particles also determined their sensitivity to the forces governing their dynamics. Depending on their mass, they were found to exhibit three types of dynamics, from dynamical mode-locking with chaotic windows, through to a typical dc response, to essentially a free-particle response. Examination of this dynamics in both the upforce and downforce directions showed that the system may not only exhibit hysteresis, but also that large Shapiro steps may appear in the downforce direction, even in cases for which no dynamical mode-locking occurred in the upforce direction.

DOI: 10.1103/PhysRevE.99.022206

I. INTRODUCTION

Frequency locking phenomena are the common features of nonlinear dynamical systems with competing timescales, and they appear in a wide variety of physical, chemical, and biological systems in nature, from their first observation in coupled pendulum clocks in in the 17th Century, to superconductors, periodically forced heart cells, and firing neurons [1]. Possible technological applications of one particular frequency locking phenomenon such as dynamical mode-locking or Shapiro steps, have, for years, inspired many experimental and theoretical studies in charge- and spin-density wave systems [2–6], vortex matter [7,8], irradiated Josephson junctions [9,10], superconducting nanowires [11,12], driven colloids [13,14], dynamics of skyrmions [15], etc. However, in search for the optimum way to control the dynamical mode-locking, one should keep in mind that there is one usually unwanted but often present phenomenon in nonlinear dynamical systems which is highly sensitive to the initial condition and which can affect the stability of locked states, this phenomenon is the chaos. Therefore, it would be impossible to get a complete microscopic picture of frequency locking without studying the chaotic behavior.

A model that can be very successful in capturing the essence of frequency locking is the dc+ac driven Frenkel-Kontorova (FK) model [16,17]. Introduced initially to describe dynamics of crystal lattice near dislocations, today, it represents one of the fundamental models in nonlinear physics due to its applicability to model many physical phenomena [16]. The standard Frenkel-Kontorova model represents a chain of harmonically interacting particles subjected to a sinusoidal substrate potential [16]. It describes different commensurate or incommensurate structures that under an external driving force exhibit a very rich response. In the presence of an external dc+ac driving force, in general, the steady-state dynamics, like those of the Josephson junction, may include chaotic, quasiperiodic, and mode-locked solutions [18]. The chaotic dynamics is characterized by a pseudorandom response of the particles to the driving forces. In their quasiperiodic state, the particles respond more or less regularly to the drive, though this response is strictly nonperiodic. Finally, the mode-locked solutions are strictly periodic, and it is mainly these that lead to the appearance of the well-known staircase macroscopic response or the Shapiro steps in the response function $\bar{v}(\bar{F})$ of the system [19–21]. The steps are called harmonic if the locking appears at integer multiples of the ac frequency, while for the locking at noninteger rational multiples of the ac frequency they are called subharmonic.

Both the overdamped and the underdamped FK model have been studied extensively [16,17]. However, it is interesting that while the underdamped FK model was usually related to the problems in solid-state friction, surface physics, and tribology [16,22–24], it was the *overdamped* FK model which was always exclusively associated with dynamical mode-locking and Shapiro steps in the charge-density wave (CDW) systems and the systems of Josephson junctions [16,17,19]. These systems represent typical examples of dissipative or overdamped physical systems where the inertia

could be irrelevant on physical grounds and where the long-term behavior is largely independent of how we start up the system [16,17,19]. In the charge-density wave systems, the frequency-dependent conductivity, when interpreted in terms of a classical model of pinned CDW, indicates a strongly overdamped system [2,25], while in the systems of Josephson junctions, the inertial terms can be disregarded if the capacitance of junctions is small enough [9].

It is well known that dissipative dynamical systems with competing frequencies can be described by the circle map. Depending on the coupling strength, the circle map can develop a cubic inflection point leading to the appearance of a devil's staircase and the transition to chaos [26–29]. When the coupling is below some critical value, the staircase is incomplete, i.e., there are quasiperiodic intervals between the frequency locked plateaus (steps) of periodic behavior. As coupling increases, the frequency-locked regions start to broaden, and at some critical value, they fill up all the space. Though the quasiperiodic intervals have zero measure, and the devil's staircase is said to be complete, they have nonzero fractal dimension (scaling index) which is *universal*, i.e., the same $D = 0.87$ for all the systems (at least for those described by the circle map with a cubic inflection point), and thus often considered as a constant of nature [26]. The mechanism leading eventually to chaos is the interaction between different resonances caused by the nonlinear coupling and overlapping of resonant regions when coupling exceeds certain critical value. Nevertheless, the universality of fractal dimension and the universality of this scenario have been questioned by many authors. In our previous work [30], we have shown that the overdamped FK model represented one example where this universality is broken. The dc+ac driven overdamped FK model has an interesting property: Though entirely nonchaotic, it exhibits the devil's staircase structure arising from the complete mode locking with the fractal dimension which varies with the system parameters. The absence of chaos was attributed to the dissipative character of the system and the Middleton no-passing rule [31,32], which applies on the strictly overdamped systems with convex interatomic interaction, and according to which the order of particles must be preserved in dynamics.

However, the discrete FK model is not integrable, and in general, its dynamics can be chaotic [16]. Due to nonintegrability, atomic motion is always accompanied by energy exchange between different modes leading to intrinsic chaotization of its dynamics [16]. Also, frequency locking in diverse physical systems, from oscillating Josephson junctions to periodically forced chicken heart cells, is intimately associated with the onset of chaotic behavior [18,26–28,33]. Appearance of chaos have been observed in numerous experimental and theoretical works in Josephson junctions and other physical systems related to the Frenkel-Kontorova model [34–37]. A good overview of the past studies can be found in Refs. [34,35,37] and references therein. Through years, the standard overdamped FK model [38,39] as well as its generalized forms [40–42] have been very successful in the studies of Shapiro steps, but all these models are entirely nonchaotic, and no chaotic dynamics has been ever observed [17,30,43]. Is it possible then, to make the FK model generally applicable and reliable for the studies of potentially chaotic systems, and can the dc+ac driven FK model exhibit chaos?

In contrast to all previous works on the Shapiro steps in the FK model, which always have been performed on some forms of an overdamped dynamics [17,30], in this paper, we extend our investigation to the underdamped Frenkel-Kontorova model driven by dc+ac forces. We will start from the well known results of the Shapiro steps observation in the overdamped standard FK mode [17,19,20], and examine the most interesting inertial effects that appear as the mass of particles is increased, and the system transfers from the overdamped to underdamped dynamics. New phenomena such as the introduction of new subharmonic steps, appearance of chaos, and hysteresis, initially nonexistent in the overdamped regime, will start to appear.

The paper is organized as follows. The model is introduced in Sec. II, while the simulation results are presented in Secs. III–VI. Appearance of subharmonic steps as one of the inertial effects is presented in Sec. III. Chaotic behavior was investigated in Sec. IV. Motion of particles and influence of their mass on the response to the dc+ac driving force is examined in Sec. V. Hysteresis and dynamics in decreasing force situations are analyzed in Sec. VI. Finally, Sec. VII concludes the paper.

II. MODEL

We consider the dynamics of the standard *damped* FK model which consists of a series of coupled harmonic oscillators u_l of mass m, subjected to the periodic substrate potential $V(u)$:

$$V(u) = \frac{K}{(2\pi)^2}[1 - \cos(2\pi u)], \tag{1}$$

where K is the pinning strength.

The system is driven by dc and ac forces,

$$F(t) = F_{dc} + F_{ac}\cos(2\pi\nu_0 t), \tag{2}$$

where F_{ac} and ν_0 are amplitude and frequency of the ac force, respectively.

The dynamics is described by the following set of equations:

$$\begin{aligned} \dot{u}_l &= v_l, \\ m\dot{v}_l &= u_{l+1} + u_{l-1} - 2u_l - \frac{K}{2\pi}\sin(2\pi u_l) - v_l + F(t), \end{aligned} \tag{3}$$

where $l = 1, ..., N$ labels the particles. The damping is fixed by two parameters m and K, and for some constant force F, the system is overdamped for (for more details see Appendix) [44,45]

$$0 < m \leqslant \frac{1}{4(2+K)}. \tag{4}$$

When the system is driven by a periodic force, two frequency scales appear in the system: the frequency ν_0 of the external periodic (ac) force and the characteristic frequency of the particle motion over the periodic substrate potential driven by the average force $\bar{F} = F_{dc}$. The competition between these two frequency scales can result in the appearance

of dynamical mode locking. The solution of the system Eq. (3) is called resonant if the time average mean velocity $\bar{v}$ satisfies the relation:

$$\bar{v} := \left\langle \frac{1}{N}\sum_{i=1}^{N} v_i \right\rangle_t = \frac{i\omega + j}{s}\nu_0, \tag{5}$$

where i, j, s are integers and ω is the winding number [19] which is fixed to rational or irrational values, characterizing commensurate or incommensurate structures, respectively. During their motion, the particles advance $i\omega + j$ sites during s cycles of the ac force; therefore, s represents the period of the solution, measured in the cycles of the ac force [18]. When $s = 1$, the solution corresponds to harmonic steps. If $s > 1$, then the solution is subharmonic (it includes components at the subharmonics of the ac force), and in this case, the motion is characterized by the appearance of a sequence which consists of s cycles of the ac force. Though the motion is different on each of s cycles that form the sequence, this sequence can repeat indefinitely.

In the case of a commensurate structures that we will study, the resonant velocity simplifies to the form

$$\bar{v} = \frac{i}{s}\omega\nu_0, \tag{6}$$

where the ratio $\frac{i}{s}$ marks harmonic and subharmonic steps ($\frac{i}{s} = \frac{1}{1}, \frac{2}{1}, \frac{3}{1}$, ... for the first, second, and third harmonic, while $\frac{i}{s} = \frac{i}{2}$ for halfinteger steps).

It is well known that in all frequency-locking systems, resonances always appear following specific order. In the dc+ac driven FK model, all observable subharmonic Shapiro steps belong to various Farey sequences without exceptions [46]. The average velocity as a function of average driving force exhibits the devil's staircase of infinite but countable steps (resonances), which can be reproduced by continued fractions formula [30,47,48]:

$$\bar{v} = \left(i \pm \frac{1}{j \pm \frac{1}{k \pm \frac{1}{l \pm \ldots}}} \right)\omega\nu_0, \tag{7}$$

where $i, j, k, \ldots$ are positive integers. Harmonic steps are presented by the first-level terms, which involve only i, while the other terms involving other integers describe subharmonic or fractional steps. Terms involving i and j are called second-level terms, those with i, j, and k are third-level terms, etc. Therefore, between any two steps there is an infinity of steps, and this progressive generation of subharmonic steps within devil's staircase is a manifestation of its self-similarity [26].

The above system of Eqs. (3) has been integrated for the commensurate structures $\omega = \frac{1}{2}$ and 1 using the fourth-order Runge-Kutta method with the periodic boundary conditions for the system of $N = 8$ particles (all parameters except m were set to the same values as in Ref. [20]). Though the winding number ω does not enter explicitly into the Eqs. (3), it is required to solve the system of equations numerically under the assumed initial as well as periodic boundary conditions. For the initial condition, at the zero applied force, we consider all particles to be at rest and equally distributed over the potential with $u_l = l\omega$ and $v_l = 0$, where $l = 1, ..., N$. In the numerical settings of the Eqs. (3), the periodic boundary conditions are implemented as $u_0 = u_N - N\omega$ and $u_{N+1} = u_1 + N\omega$. The timescale ν_0^{-1} imposed by the periodic driving force $F(t)$ has been used. The force has been increased from zero with the very fine discretization $10^{-4} - 10^{-6}$. Unlike in the overdamped case, here, the behavior of the system depends on its previous history therefore, the initial condition at the each step of driving force was obtained from the last step in the integration, at its previous value.

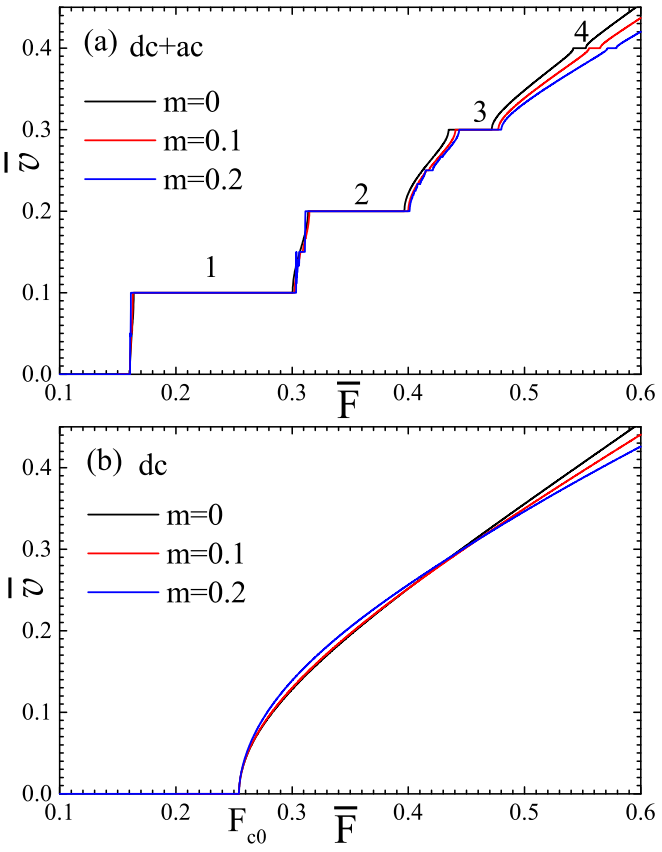

FIG. 1. The average velocity $\bar{v}$ as a function of the average driving force $\bar{F}$ for $K = 4$, $\nu_0 = 0.2$, $F_{ac} = 0.2$, $\omega = \frac{1}{2}$, and different values of the mass $m = 0, 0.1$ and 0.2 represented by different colors. The case $m = 0$ corresponds to the standard overdamped case. Results in (a) and (b) corresponds to the dc+ac and dc driven dynamics, respectively. Numbers mark the harmonic steps, while F_{c0} marks dynamical dc threshold.

III. INERTIAL EFFECTS AND THE ORIGIN OF SUBHARMONIC STEPS

We will start from the well known result of Shapiro steps observation in the standard overdamped FK model with commensurate structure $\omega = \frac{1}{2}$ presented in Ref. [20], and examine how the increase of mass affects its dynamic. In Fig. 1, the average velocity as a function of the average driving force is presented for various values of mass m. For the comparison we present the results for both cases: dc+ac, and dc driven FK model in Figs. 1(a) and 1(b), respectively. As m increases, even at this resolution we could see in Fig. 1(a) that halfinteger steps start to appear, and the transition regions between harmonic steps are attaining staircase structure. In

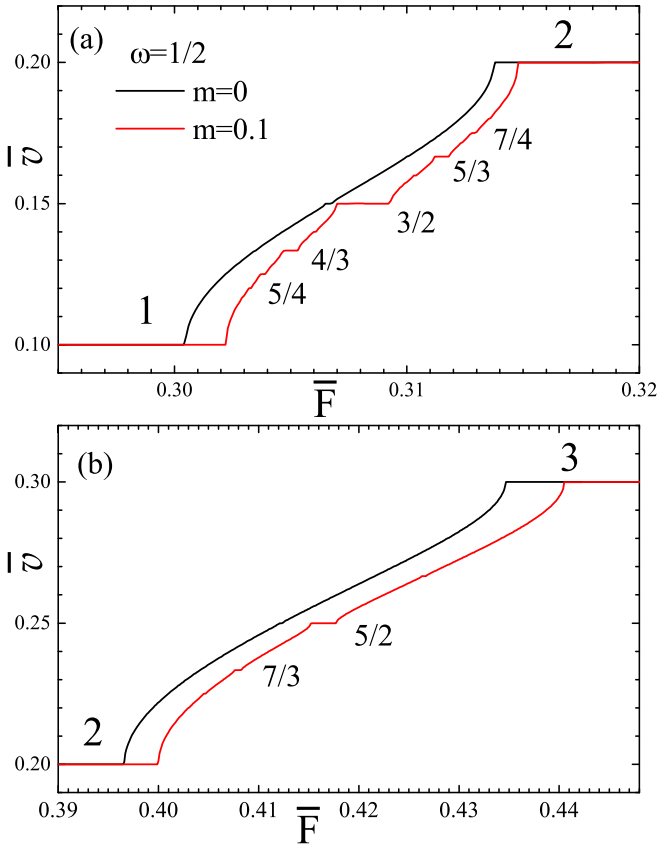

FIG. 2. The average velocity $\bar{v}$ as a function of the average driving force $\bar{F}$ for $m = 0.1$ in the region between the first and the second harmonic step in (a), and in the region between the second and the third harmonic step in (b). The rest of parameters are the same as in Fig. 1.

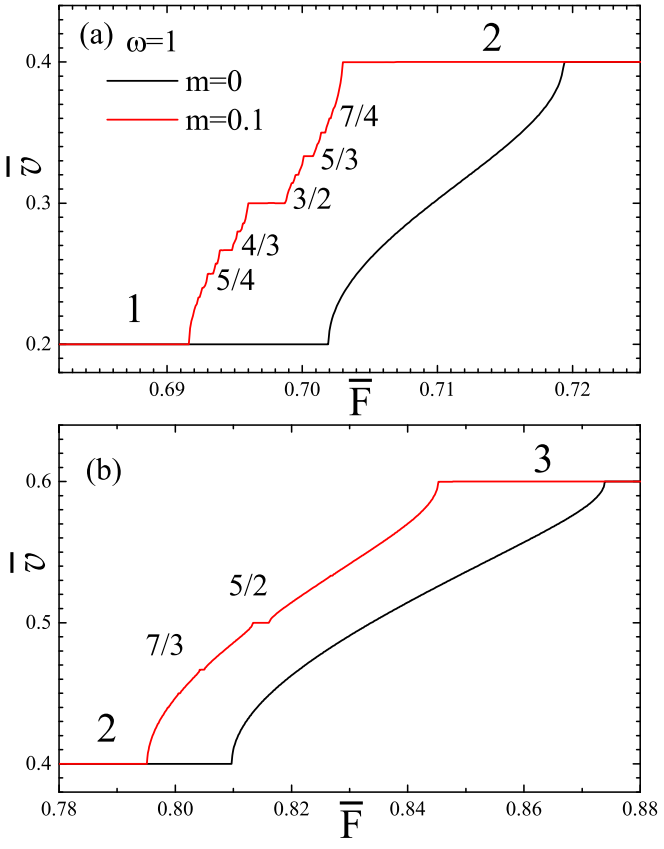

FIG. 3. The average velocity $\bar{v}$ as a function of the average driving force $\bar{F}$ for $\omega = 1$, and $m = 0$, and 0.1 in the region between the first and the second harmonic step in (a), and in the region between the second and the third harmonic step in (b). The rest of parameters are the same as in Fig. 1.

the absence of external periodic force in Fig. 1(b), there is no locking and though the curve start to shift from the case $m = 0$, the response is still typical for the overdamped dc driven systems. If we look at the depinning point, we could see that critical depinning force is not affected by the increase of mass. The critical depinning force for the dc driven system is also called dynamical dc threshold, it is determined by the properties of the substrate potential and the commensurability of the system [16], and in our case it has the value $F_{c0} = 0.2544$.

In Fig. 2, the high resolution plots of the region between the first and the second harmonic step, and the region between the second and the third harmonic step are shown. As we can see, the subharmonic steps appear following continued fraction formula Eq. (7). According to the Farey rule [46], the largest one are halfinteger steps $\frac{3}{2}$ and $\frac{5}{2}$, which are followed by higher order subharmonic steps $\frac{4}{3}$, $\frac{5}{3}$, $\frac{5}{4}$, $\frac{7}{4}$, and $\frac{7}{3}$ in Figs. 2(a) and 2(b), respectively.

We have also examined the trivial case $\omega = 1$ for which, in the strictly overdamped case, the system reduces to the single particle model and no subharmonic locking exists [16]. In Fig. 3, the high resolution plots of the region between the first and the second harmonic step, and the region between the second and the third harmonic step for $\omega = 1$ are presented. The results clearly show presence of the whole series of subharmonic steps.

We substantiate our claim of subharmonic step generation via inertia by computing the fractal dimension D (definition can be found in Refs. [26] and [30]). In particular, starting from strictly overdamped regime $m = 0$ via equations of motion as in Ref. [30], and $m > 0$ via Eq. (3), we proceed to compute the fractal dimension D from the response function $\bar{v}(\bar{F})$. If we focus on the region between the first and the second, and the region between the second and the third harmonic steps, in Figs. 4(a) and 4(b), D is computed for parameter regimes presented in Figs. 2 and 3, respectively. At $m = 0$, the fractal dimension should be 1 or close to that value (up to the numerical precision) due to the absence of any subharmonic mode locking. By increasing the mass (inertial term), the subharmonic steps start to appear, and accordingly, the fractal dimension indeed goes below 1, indicating the complete locking and the devil's staircase structure [30].

The origin of subharmonic steps in the frequency locking systems has been a matter of many debates [17]. In the standard overdamped FK model ($m_i = 0$), it was proved that subharmonic steps do not exist for integer values of ω [49,50]. For rational noninteger values of ω, the subharmonic steps appear, however, their size is so small that they are hardly visible on the regular plot $\bar{v}(\bar{F})$ [20]. Therefore, the

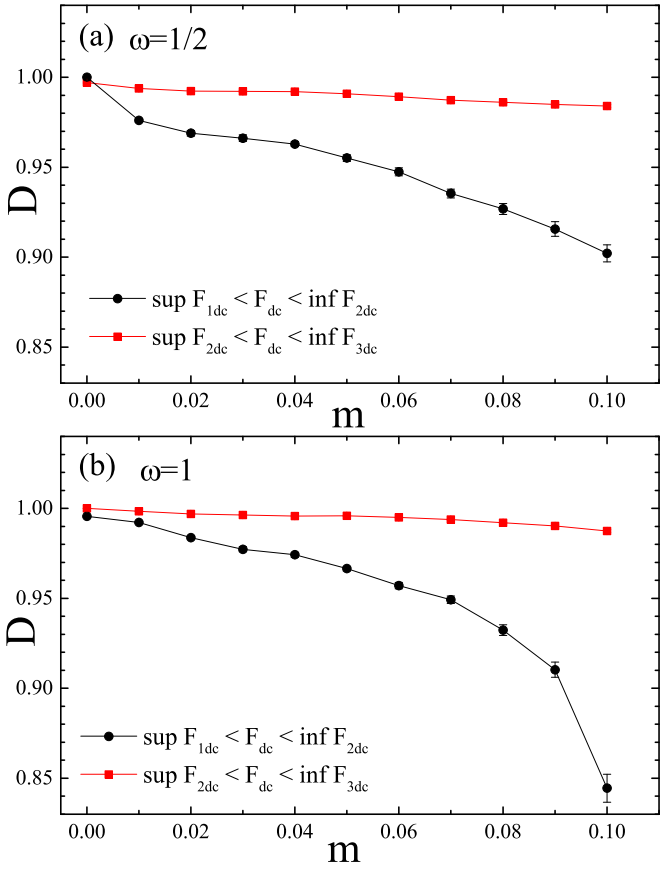

FIG. 4. Fractal dimension D as a function of mass m measured in the region between the first and the second ($F_{1dc} < F_{dc} < F_{2dc}$), and the second and the third ($F_{2dc} < F_{dc} < F_{3dc}$) harmonic steps for $\omega = \frac{1}{2}$, and 1 in (a) and (b), respectively. The rest of the parameters are the same as in Fig. 1.

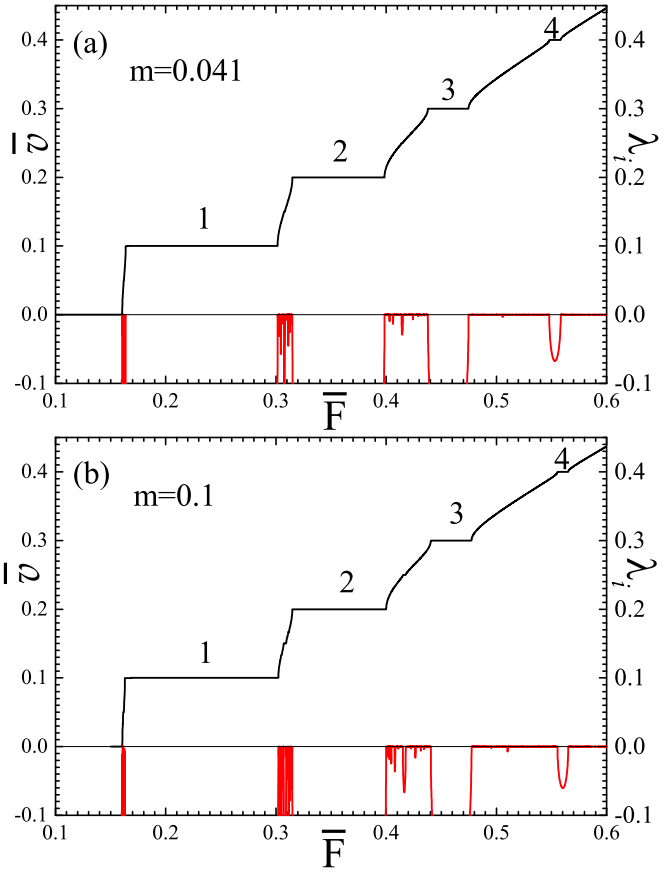

FIG. 5. The average velocity $\bar{v}$ as a function of the average driving force $\bar{F}$ and the corresponding Lyapunov exponents λ_i for $K = 4$, $F_{ac} = 0.2$, $\nu_0 = 0.2$, $\omega = \frac{1}{2}$, and $m = 0.041$ and 0.1 in (a) and (b), respectively. On this scale of y axis only the largest Lyapunov exponent is visible. Numbers mark the harmonic steps.

standard overdamped FK model could not be used for modeling phenomena related to subharmonic steps. However, it was shown in Ref. [40] that even the strictly overdamped FK model can exhibit large half integer and the whole series of subharmonic steps due to deformation of substrate potentials in any commensurate structures, regardless of the value of winding number ω [17]. However, here, in Figs. 2–4, the subharmonic steps appear in the standard FK model with sinusoidal potential, and their origin comes from the presence of inertial term. These results, together with the previous one in Ref. [40] clearly show that there is no one universal scenario behind the appearance of subharmonic steps but they may equally exist in both overdamped or underdamped systems and have different origins such as deformation of the potential as it was shown previously or inertial effects in this case.

IV. THE APPEARANCE OF CHAOS

The increase of mass in the ac+dc driven FK model may have much more dramatic effects than just simply inducing subharmonic mode-locking. According to Eq. (4), for $K = 4$, our system is overdamped if $m < m_c = 0.0417$, and it can exhibit devil's staircase and complete locking while remaining completely nonchaotic [30]. In our search for chaotic behavior we will apply the Lyapunov exponent (LE) computational technique [30,43] and extend our examination further into the underdamped region. We have calculated the Lyapunov exponent spectrum which for the system Eqs. (3) consists of $2N$ equations, where each LE is associated with each independent coordinate of the system. In nonlinear dynamical systems, the Lyapunov exponents determine degree of chaos inherent to the system and quantify the sensitivity of the system to the initial conditions. Starting from some small arbitrary initial separation, positive or negative value of the particular LE characterizes the long term average exponential divergence or convergence of the coordinate. If only one LE is positive, the system is chaotic, while for more than one positive LE, it is hyperhchaotic.

In Fig. 5, the response function $\bar{v}(\bar{F})$ and the corresponding Lyapunov exponents λ_i are presented for two cases: $m < m_c$ and $m > m_c$ in Figs. 5(a) and 5(b), respectively. As we can see, the increase of m, and just the crossing of the overdamped limit m_c did not change much the LE which clearly show that the system does not have to be necessarily strictly overdamped to be nonchaotic.

However, further increase of mass will completely change the motion of particles. In Fig. 6, the response function

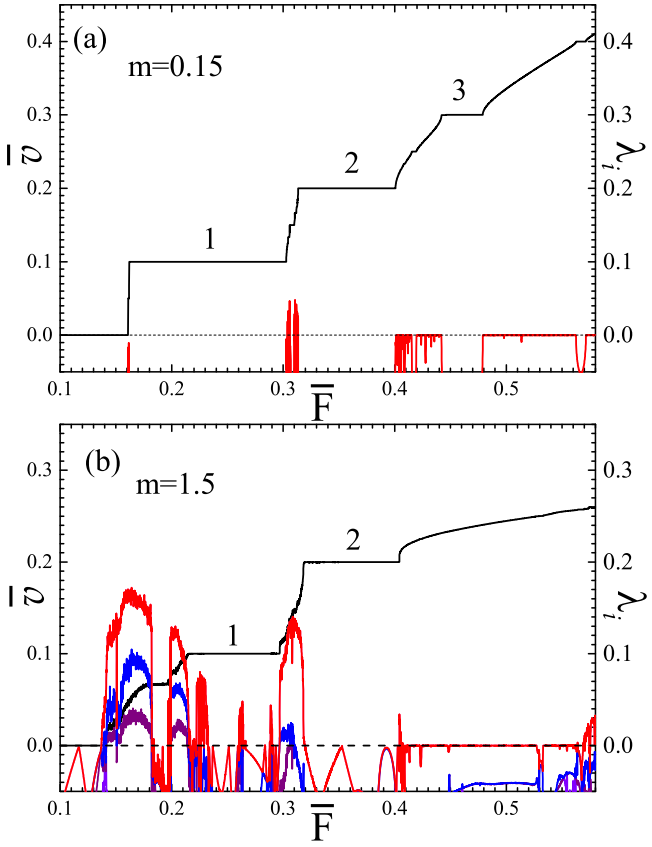

FIG. 6. The average velocity $\bar{v}$ as a function of the average driving force $\bar{F}$ and the corresponding Lyapunov exponents λ_i for $m = 0.15$ and 1.5 in (a) and (b), respectively. The rest of parameters are the same as in Fig. 1. On this scale of y axis only the largest Lyapunov exponents are visible. Numbers mark the harmonic steps.

$\bar{v}(\bar{F})$ and the corresponding Lyapunov exponents (LE) λ_i are presented for much larger values of m. The positive values of the LE indicate the presence of chaotic behavior. For small m such as in Fig. 6(a), the chaotic motion appears between the first and the second harmonic, while as m increases in Fig. 6(b), the chaos is spread in all regions between large harmonic steps. In the same way as the positive values of the LE mark the chaotic motion, the negative values, however, mark the Shapiro steps, i.e., the locked regions with periodic motion of particles.

Further, we will focus on the chaotic regions between the large harmonic steps and examine in detail the onset on chaos on subharmonic steps for two values of mass: $m = 0.2$ and 1.25. In Fig. 7, the staircase structure of the average velocity as a function of the average driving force $\bar{v}(\bar{F})$ for $m = 0.2$ is presented. If we focus, for example, on the region between second and the third step in Fig. 7(a), the high resolution analysis with the force step $\Delta F = 10^{-6}$, in Figs. 7(b) and 7(c), reveals an infinite series of subharmonic steps which appear following continued fraction formula Eq. (7). Further increase of resolution will reveal an interesting structure, in Fig. 7(d), we can see that the subharmonic steps are separated by chaotic windows.

To examine this interesting structure we perform the LE analysis. In Fig. 8, the high resolution plot of the response

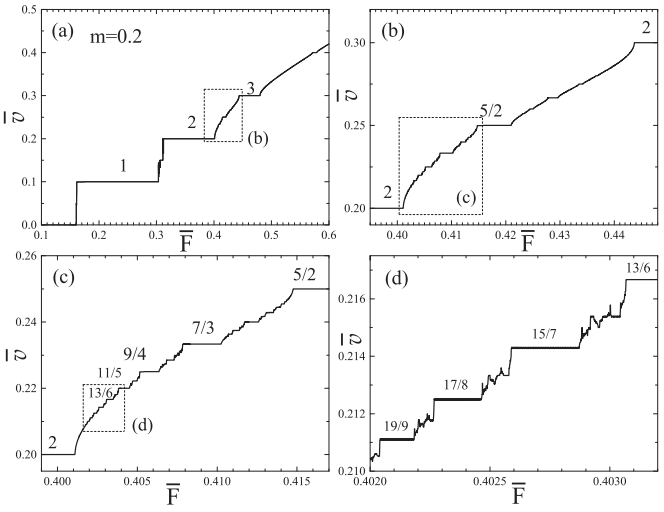

FIG. 7. The average velocity as a function of the average driving force $\bar{v}(\bar{F})$ for $m = 0.2$, $K = 4$, $F_{ac} = 0.2$, $\nu_0 = 0.2$, and $\omega = \frac{1}{2}$. Numbers mark harmonic and subharmonic steps. The staircase in (b), (c), and (d) represent the high-resolution views of the selected areas in (a), (b), and (c), respectively.

function and the Lyapunov exponents in the region which is situated between the second and third harmonic is presented. As we can see the subharmonic steps are separated by chaotic windows indicated by the positive Lyapunov exponent.

Devil's staircase containing Shapiro steps separated by self-similar chaotic regions has been observed both in the single and in the one dimensional stack of Josephson junctions [34,35]. It was shown that in the current-voltage characteristics of the junctions the staircase with chaotic intervals preserves the scaling of the original staircase with the fractal dimension close to 0.87. Considering the fact that the

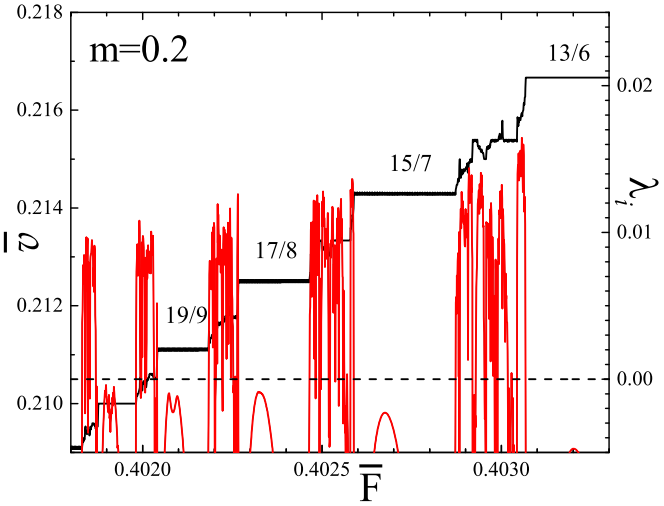

FIG. 8. The Lyapunov exponents λ_i as a function of the average driving force $\bar{F}$ and the corresponding response function $\bar{v}(\bar{F})$ in the small region between the second and the third harmonics for $m = 0.2$ are presented. On this scale of y axis only the largest Lyapunov exponent is visible. The rest of the parameters are the same as described in the caption of Fig. 7.

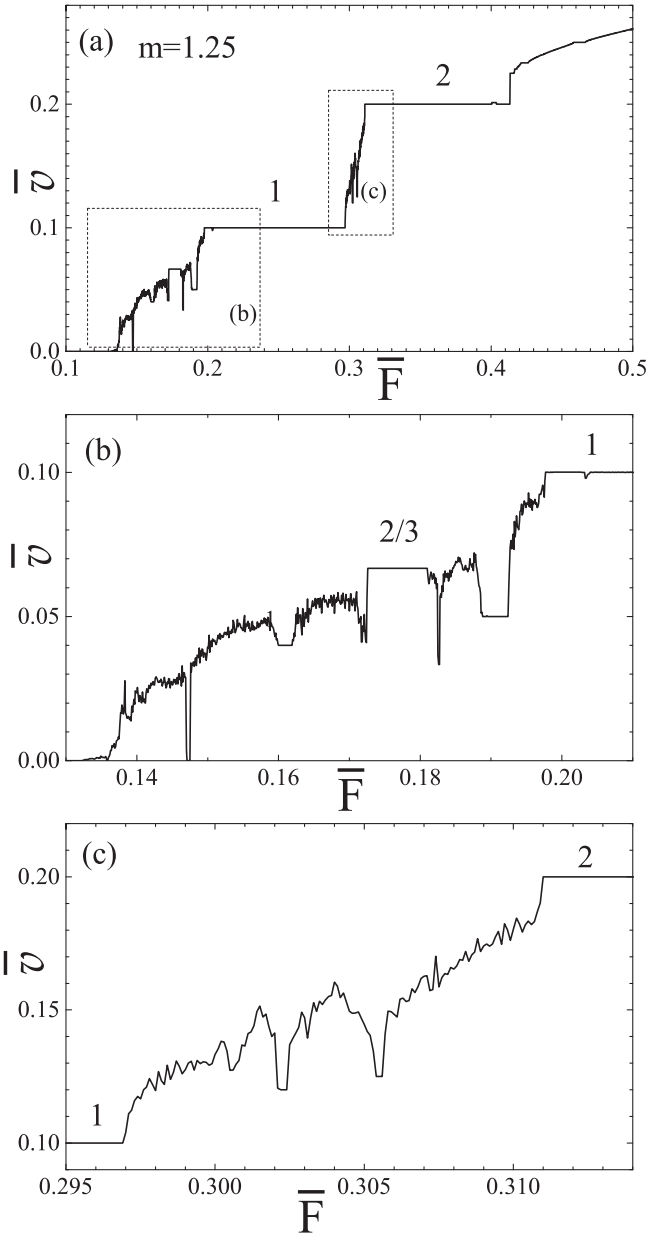

FIG. 9. The average velocity as a function of the average driving force $\bar{v}(\bar{F})$ for $m = 1.25$, $K = 4$, $F_{ac} = 0.2$, $\nu_0 = 0.2$, and $\omega = \frac{1}{2}$. Numbers mark harmonic and subharmonic steps. The staircase in (b) and (c) represent the high-resolution views of the selected areas in (a).

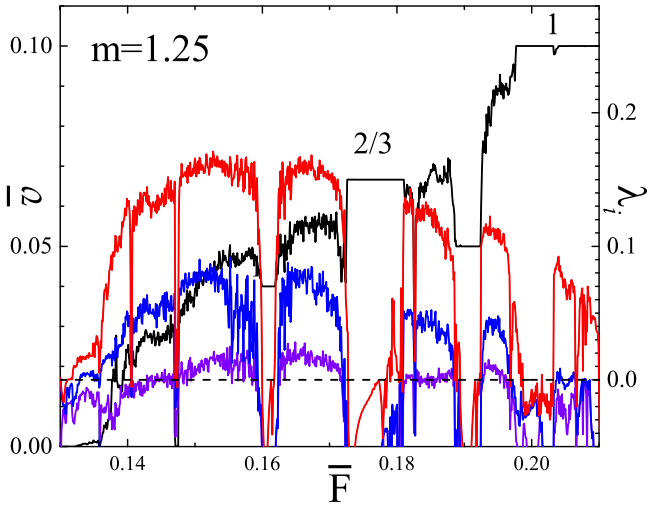

FIG. 10. The Lyapunov exponents λ_i as a function of the average driving force $\bar{F}$ and the corresponding response function $\bar{v}(\bar{F})$ in the region between the zero and the first harmonicstep for $m = 1.25$ are presented. Different colors of λ_i corresponds to different Lyapunov exponents. The rest of the parameters are the same as described in the caption of Fig. 9.

overdamped FK model also exhibits complete locking [30] raises the question whether this staircase of subharmonic steps separated by chaotic windows which appears in the underdamped case is still complete and how its scaling changes. To estimate the fractal dimension D we have followed the same method used in Ref. [30], and for the region between the second and third harmonic step, obtained $D = 0.8759$ with an uncertainty of ± 0.0166.

The increase of mass to larger values will affect significantly the existence of Shapiro steps. In Fig. 9, the staircase structure of the average velocity as a function of the average driving force $\bar{v}(\bar{F})$ for $m = 1.25$ is presented. As the mass increases, the locking appears only at the lower values of force. Unlike the case in Fig. 7(a) where three harmonics appear, here in Fig. 9(a), only two harmonics can be observed, and as the force increases to higher values, dynamical mode-locking disappears. High resolution examination of the regions between harmonic steps in Figs. 9(b) and 9(c) shows that only some of subharmonic steps can be observed, and the staircase structure with the subharmonic steps as it was in Fig. 7, is now completely destroyed. Calculation of fractal dimension showed disappearance of complete locking as D approached 1.

We further extend our analysis of the results in Fig. 9 to the calculation the Lyapunov spectrum. In Fig. 10, the Lyapunov exponents for the region between the zero and the first harmonic is presented. More than one positive LE clearly indicates the presence of hyperchaos.

V. MOTION OF PARTICLES: FROM LIGHT TO HEAVY

When a particle moves in the dc+ac driven FK model, its motion is governed by the simultaneous action of the pinning force from the substrate potential, dc driving force, and the time periodic ac force. If the system is not overdamped and the inertial term is present, then the mass of particle will determine its sensitivity to those forces and the way it moves.

In Fig. 11, the evolution of the response function $\bar{v}(\bar{F})$ with the increase of mass is presented. For the mass $m = 0.2$ in Fig. 11(a), as the force increases, Shapiro steps appear at the lower values of driving force, and with the further increase of $\bar{F}$, the curve approaches to the response of the dc ($F_{ac} = 0$) driven system represented by the dashed line. The critical depinning force F_c for the dc+ac curve is much lower than dynamical dc threshold F_{c0} [17]. We already showed in the previous section that the increase of mass would start destroying the staircase, and as we can see here in Fig. 11(b),

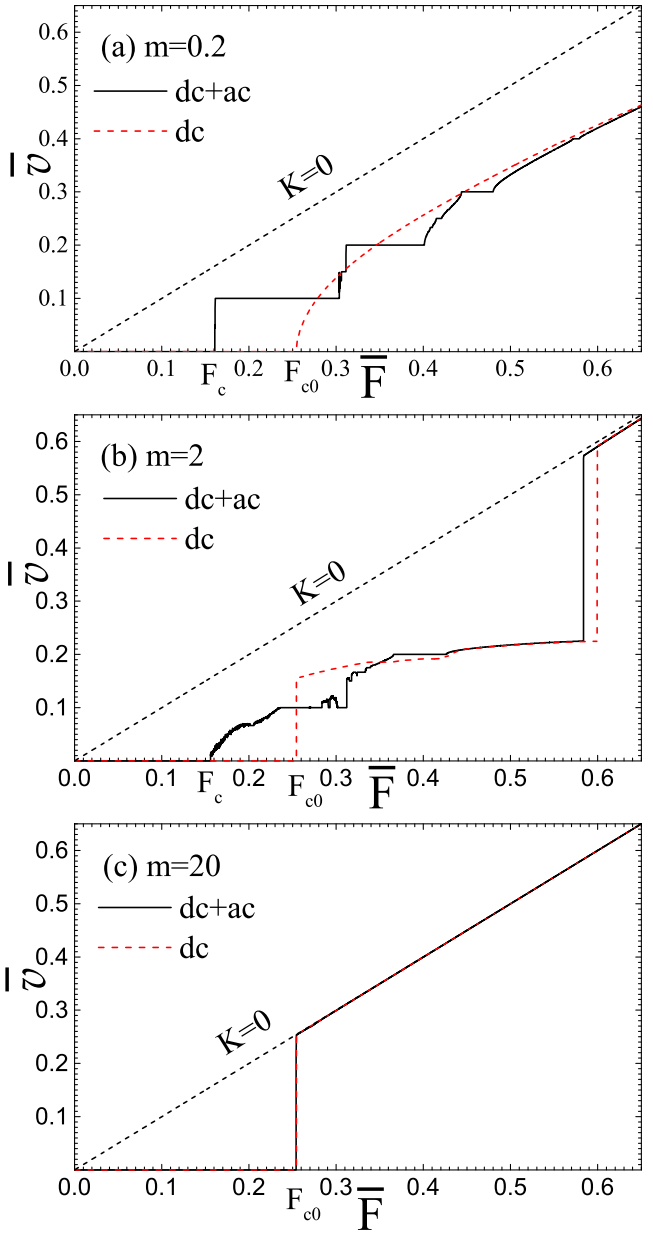

FIG. 11. The average velocity as a function of the average driving force $\bar{v}(\bar{F})$ for $K = 4$, $F_{ac} = 0.2$, $\nu_0 = 0.2$, $\omega = \frac{1}{2}$, and $m = 0.2$, 2, and 20 in (a)–(c), respectively. The dc curve presented by the red dashed line corresponds to the dc driven system where $F_{ac} = 0$, while $K = 0$ is linear response of the system of free particles. F_c and F_{c0} mark critical depinning force and dynamical dc threshold, respectively.

only two large harmonic steps separated by the chaotic regions are visible. As $\bar{F}$ increases and the mode-locking disappears, the response $\bar{v}(\bar{F})$ approaches to the one of the dc driving system, and goes to the response of free particles ($K = 0$) for very large $\bar{F}$. If we increase mass to even larger values in Fig. 11(c), regardless of the ac amplitude, we have a typical dc response, particles depin at F_{c0}, and move with the velocity which is now a linear function of driving force. Namely, when particles become heavy, they respond more slowly to the ac force, in the same way as they respond more slowly if the ac frequency is increased. From the dynamics of overdamped FK model [17] we know that if we increase the ac frequency, at some values, particles became unable to follow the ac drive and become insensitive to it. Hence, particles become insensitive to the periodic ac force, which therefore, does not play any role in the dynamics, and the system behaves as the dc driven system. For small masses such as in Fig. 11(a), the system is always far from the system of free particles presented by the $K = 0$ curve. However, for larger m, not only that particles become insensitive to the ac force, but above certain values of $\bar{F}$ which is around 0.58 in Fig. 11(b), or even immediately after depinning at F_{c0} in Fig. 11(c), the substrate potential will have no influence, and they become free.

According to the results in Figs. 11(a)–11(c), we can clearly distinguish different regions where particles exhibit one of the three different types of dynamics:

(i) *the dc+ac driven*, where particles are sensitive to the both dc and ac forces while moving over the substrate potential, and the staircase structure of Shapiro steps with possible chaotic behavior occurs;

(ii) *the dc driven*, where particles become insensitive to the ac force, and the response $\bar{v}(\bar{F})$ is the one typical for dc driven underdamped FK model;

(iii) *the free particles*, where particles do not feel substrate potential and move freely with a speed which increases linearly with $\bar{F}$.

These results together with those in previous section clearly show that though the increase of mass may induce subharmonic steps and chaotic behavior which otherwise in overdamped limit would not exist, the further increase will actually have contra effect by reducing the mode-locking and destroying the staircase at very large values of m. Since the chaotic behavior is closely related to the instability of periodic solutions i.e. steps, it will appear only in the certain range of driving force and system parameters where the steps also appear.

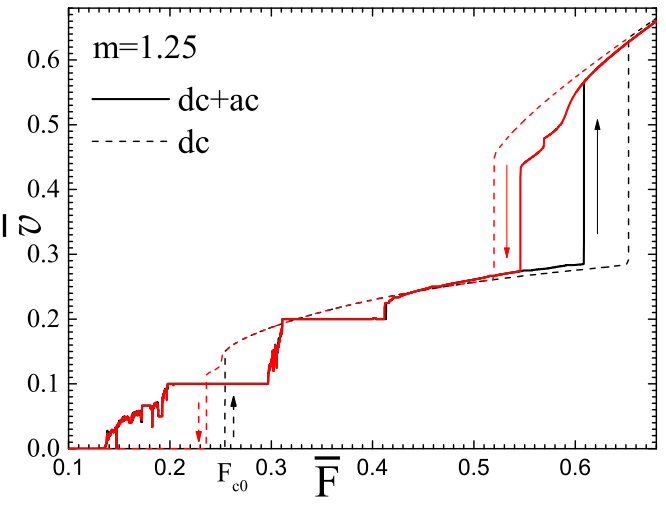

FIG. 12. The average velocity $\bar{v}$ as a function of the average driving force $\bar{F}$ for $K = 4$, $\omega = \frac{1}{2}$, $F_{ac} = 0.2$, $\nu_0 = 0.2$, and $m = 1.25$. The dashed lines corresponds to the dc driven case where $F_{ac} = 0$. F_{c0} marks dynamical dc threshold.

VI. HYSTERESIS AND SHAPIRO STEPS

One phenomenon which is inherent to underdamped nonlinear systems is hysteresis. In the overdamped FK model, dynamics does not depend on previous history, and in the studies of overdamped dynamics, the force is usually varied in the increasing (upforce) direction. So, we followed the same fashion in this study, and all results presented in previous sections are obtained by increasing force from zero. However, unlike in the overdamped case, here, the previous history determines the response, and the system may have running solutions even if the minima of the potential still exist. Namely, due to their momentum the particles may overcome the next barrier which is lower than the one from which they were falling due to the dc force contribution which gives the potential a washboard shape. Depending on their initial velocity or momentum, for the same value of driving force the particles may be either moving or pinned, i.e. the system exhibits bistability which will result in the appearance of hysteresis in the response function $\bar{v}(\bar{F})$. Hysteresis has been studied extensively in both one-dimensional and two-dimensional dc driven FK model and its generalizations [51–54], where it was shown that transition from the locked to the sliding state passed through hierarchy of hysteretic depinning transitions, where hysteresis persisted even in the presence of thermal noise.

In this section we will examine the appearance of hysteresis in the dynamics of the dc+ac driven underdamped FK model. Parameter which again plays the major role is of course the mass. For the case $m = 0.2$, which was presented in Fig. 7, hysteretic transitions are invisible on regular plots, therefore, we will not show this case. Nevertheless, the situation will change as the mass increases. In Fig. 12, the average velocity $\bar{v}$ as a function of the average driving force $\bar{F}$ for $m = 1.25$ is presented. For the comparison, we also presented the curves (dashed lines) for the dc driven case. Unlike the dc driven case where all transitions are characterized by the large hysteresis, in the dc+ac driven dynamics, a large hysteresis appears in the region of large driving force where particles become insensitive to the ac force and move more like in dc driven system.

As we already know, further increase of mass as it was shown in Fig. 11, will destroy the staircase and the Shapiro steps. In Fig. 13, the hysteresis in the response function $\bar{v}(\bar{F})$ for $m = 5$ is presented. In the upforce direction in Fig. 13(a), there is no mode-locking except the very small subharmonic step $\frac{4}{3}$, which is visible in Fig. 13(b), and the particles move as in the dc driven case. However, an interesting phenomenon

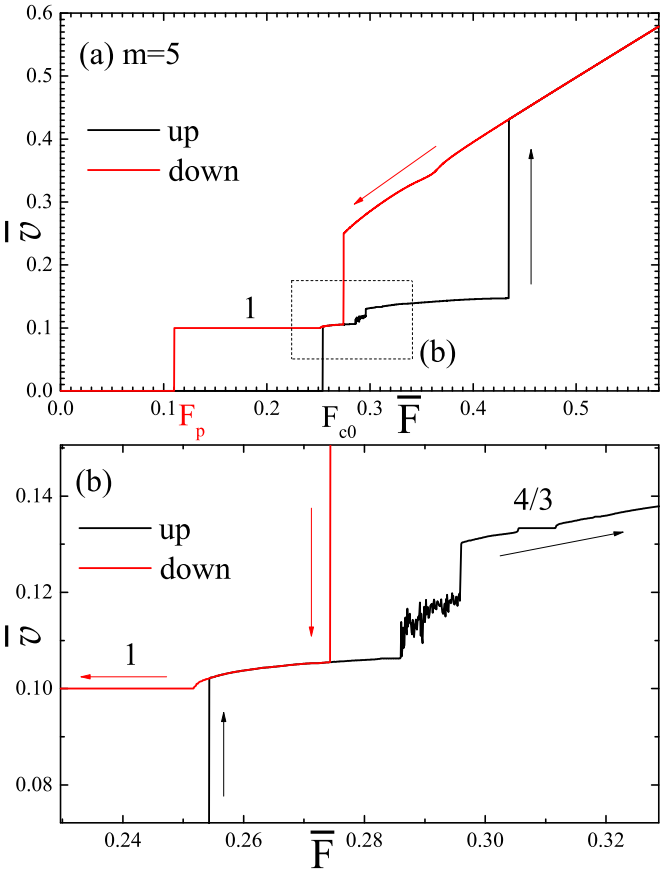

FIG. 13. The average velocity $\bar{v}$ as a function of the average driving force $\bar{F}$ for $m = 5$, $K = 4$, $\omega = \frac{1}{2}$, $F_{ac} = 0.2$, and $v_0 = 0.2$. The high-resolution view of the selected area in (a) is presented in (b) where the numbers mark Shapiro steps. $F_{c0} = F_c$ marks critical depinning force or dynamical dc threshold while F_p represents critical pinning force in downforce direction.

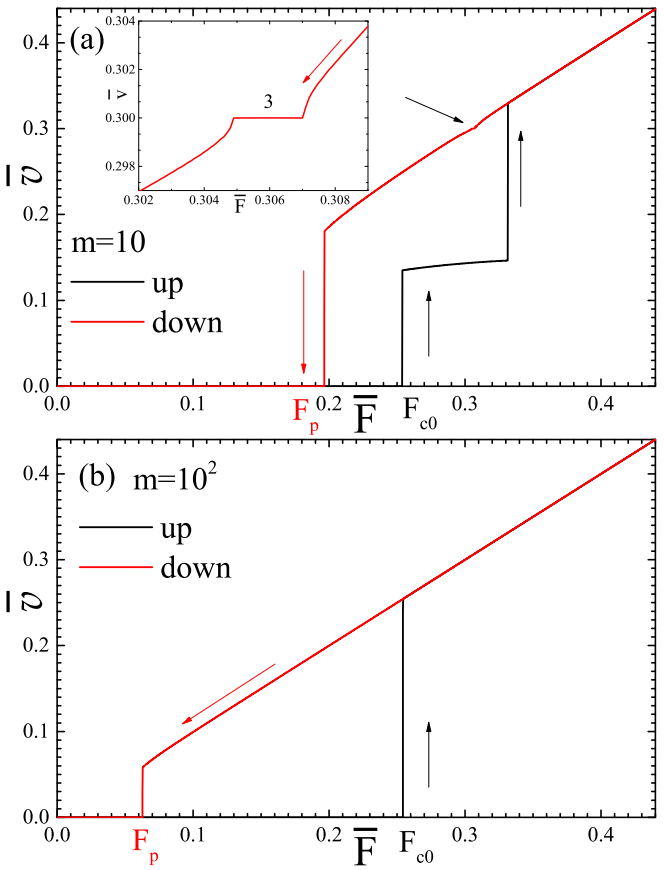

FIG. 14. The average velocity $\bar{v}$ as a function of the average driving force $\bar{F}$ for $K = 4$, $\omega = \frac{1}{2}$, $F_{ac} = 0.2$, $v_0 = 0.2$ and $m = 10$ and 10^2 in (a) and (b), respectively. $F_{c0} = F_c$ and F_p mark the critical depinning and pinning force, respectively. Inset shows the third harmonic step which appears in the downforce direction.

appears in the downforce direction, as the force passes the critical depinning force F_{c0}, the particles lock to the external ac frequency, and the large first harmonic step appears.

In Fig. 14, the evolution of hysteretic behavior with the increase of m to very large values is presented. Here for $m = 10$, again in the downforce direction, a very small third harmonic step shown in the Inset of Fig. 14(a) is observed. This is yet another example of "downforce" Shapiro step in the situation where no dynamical mode-locking exist in the "upforce" direction. From the theory and studies of underdamped dynamics, we know that the kinetic energy of the preceding stage defines transition to the following stage Ref. [54]. Consequently, in the downforce direction particles will due to its momentum pass critical depinning force and enter into the region where dynamical mode-locking may appear due to their sensitivity to the ac force.

Another interesting aspect of hysteretic behavior is how critical pinning force F_p in downforce direction changes with m. In the previous section we showed that with the increase of mass, the critical depinning force F_c approaches the dynamical dc threshold F_{c0} after which in the upforce direction the system always behaves like in the dc driven case regardless of the ac force and its amplitude. However, in downforce direction as we can see for the case $m = 10^2$ in Fig. 14(b), the pinning force F_p is totally different from the case in (a) simply because the particles with larger mass will have larger momentum and therefore, be able to continue moving longer. If m increases to infinity, the critical pinning force F_p will approach to zero.

VII. CONCLUSION

In this work, we presented the major inertial effects that can appear in the dc+ac driven underdamped Frenkel-Kontorova model and that distinguish its dynamics from the overdamped case. As the mass increases and the systems transfers from the overdamped to underdamped limit, one of the immediate effects is the appearance of subharmonic steps and the staircase structure even in the commensurate systems with integer values of winding number where no subharmonic locking exists in the overdamped limit. The most striking and interesting inertial effect is certainly the appearance of chaotic behavior where depending on the mass, the systems may exhibit a staircase of Shapiro steps separated by chaotic windows which retains the fractal dimension of the original staircase. Our results also show that the mass determines sensitivity of particles to the forces which rule their motion. Namely, depending on their mass, the particles may exhibit mode-locking or become insensitive to the external ac force or even become free from the influence of the substrate potential and move with velocity which is linear function of driving force. Another interesting inertial effect is the hysteresis, i.e., not just the hysteretic behavior of the average velocity as a function of average driving force but the appearance of Shapiro steps in the downforce direction in the situation where there is no dynamical mode-locking in the upforce direction.

This work could be important for all nonlinear physical systems with competing frequencies which exhibit devil's staircase and potentially could go under the transition to chaos. Though such physical systems might come from a wide variety of physical, chemical and biological origins, their dynamics is often described by equations similar to the one in our paper. Frequency locking is basically the resonant effect between two oscillators where one of them is replaced by an external periodic driver. The presented results give a clear picture of what happens when such system slowly transfers from the overdamped to the underdamped regime by the increase of the inertial term. Thus, as a starting point in our work we used the well known result of the Shapiro steps observation in the overdamped FK model and the parameters settings which were widely used in those studies [17,19,20]. Our results clearly show how much mass and driving force we need in this particular set of parameters to have subharmonic steps, chaos, certain sensitivity to external forces, or hysteresis. The observed effects are not particular to the FK model but are general characteristics of any periodically driven, underdamped system.

The ac+dc driven FK model is well known as a model that gives a fair description of the sliding charge-density wave systems in a radio frequency field and the Josephson junction systems in a microwave field [17,19]. The chaotic behavior has already been studied in those systems [29]. In recent years, a number of studies in the Josephson junction systems has been particularly focused on the presence of one unusual phenomenon known as the structured chaos [34,35]. That is, the in-between chaotic regions interlacing the subharmonic Shapiro steps in the current-voltage characteristics of the junctions were shown to be self-similar and structured. Detail comparative analysis between chaotic behavior of the FK model and the JJs systems as well as the possibilities of reproducing the chaotic phenomena observed in those systems are on the way, and they will be published separately. Moreover, in this work we examined only the effect of inertial term but other parameters such as the ac amplitude or frequency, the shape of the potential or the type of particle interaction as well as the number of particles (the number of particles is irrelevant in the overdamped commensurate structures but not in the underdumped ones) play an important role and can trigger or suppress chaotic behavior and completely change dynamics. These problems will be also part of our future studies.

Shapiro steps represent a phenomenon with a great potential for technological applications from device building to voltage standards and detection of Majorana fermions [55]. In any application, the stability of Shapiro steps is crucial and any chaotic behavior must be avoided. This requirement is even more complicated by the fact that optimum operating region is actually at the onset of chaos. Therefore, chaotic aspects of frequency locking phenomena are interesting both theoretically and experimentally, and we hope that this as well as our further studies on this problem could help in creating a good theoretical guideline for technological applications of Shapiro steps and motivate future studies and experiments.

ACKNOWLEDGMENTS

We express our gratitude to Jovan Odavić for his expertise in programming. J. Tekić thanks Prof. Yu. M. Shukrinov and the BLTP, JINR, Dubna in Russia for their generous hospitality where a part of this work was done. This work was supported by the Serbian Ministry of Education and Science

under Contracts No. OI-171009 and No. III-45010 and by the Provincial Secretariat for High Education and Scientific Research of Vojvodina (Project No. APV 114-451-2201). The reported study was partially funded by the Russian Foundation for Basic Research (RFBR) Projects No. 18-02-00318 and No. 18-52-45011-IND and Russian Science Foundation (RSF) Project No. 18-71-10095.

APPENDIX: THE OVERDAMPED CONDITION

1. First method

According to Ref. [45], if we consider the following system of equations given as

$$m_n\ddot{x}_n + \gamma_n\dot{x}_n = f_n(x), n_n, \quad \gamma_n > 0, \tag{A1}$$

where the function $f_n(x)$ satisfies cooperativity (convex) condition

$$\frac{\partial f_n}{\partial x_j} \geqslant 0, \quad \forall j \neq n, \tag{A2}$$

the system is overdamped if

$$-4m_n\frac{\partial f_n}{\partial x_n} \leqslant \gamma_n^2. \tag{A3}$$

If this is applied on the FK model under external forces,

$$m\ddot{u}_l + \dot{u}_l = u_{l+1} - 2u_l + u_{l-1} - \frac{K}{2\pi}\sin(2\pi u_l) + F, \tag{A4}$$

then the inequalities Eqs. (A2) and (A3) become

$$-4m\frac{\partial}{\partial u_l}\left[u_{l+1} - 2u_l + u_{l-1} - \frac{K}{2\pi}\sin(2\pi u_l) + F\right] \leqslant 1, \tag{A5}$$

and

$$-4m[-2 - K\cos(2\pi u_l)] \leqslant 1. \tag{A6}$$

The left side of the inequality Eq. (A6) has maximal value when $\cos(2\pi u_l) = 1$, and in that case, the inequality becomes

$$4m(2 + K) \leqslant 1, \tag{A7}$$

or $m \leqslant \frac{1}{4(2+K)}$. Since the mass m is nonnegative, the overdamped condition is given as $0 \leqslant m \leqslant \frac{1}{4(2+K)}$.

2. Second method

Linearizing the system Eq. (A4) we obtain the following equation:

$$m\ddot{u}_l + \dot{u}_l = u_{l+1} - 2u_l + u_{l-1} - Ku_l + F, \tag{A8}$$

which can be written in the form

$$m\ddot{u}_l + \dot{u}_l + (2 + K)u_l = u_{l+1} + u_{l-1} + F. \tag{A9}$$

From Eq. (A9), the homogeneous equation

$$m\ddot{u}_l + \dot{u}_l + (2 + K)u_l = 0 \tag{A10}$$

has the characteristic equation

$$m\lambda^2 + \lambda + (2 + K) = 0, \tag{A11}$$

with the characteristic roots

$$\lambda_{1,2} = \frac{-1 \pm \sqrt{1 - 4m(2 + K)}}{2m}. \tag{A12}$$

According to Eq. (A12), the system is overdamped if $1 - 4m(2 + K) > 0$, which leads to

$$m < \frac{1}{4(2 + K)}. \tag{A13}$$

Therefore, $m_c = \frac{1}{4(2+K)}$ represents the critical damping.

[1] A. Pikovsky, M. Rosenblum, and J. Kurths, *Synchronization: A Universal Concept in Nonlinear Sciences* (Cambridge University Press, Cambridge, 2001).
[2] G. Grüner, Rev. Mod. Phys. **60**, 1129 (1988).
[3] R. E. Thorne, J. S. Hubacek, W. G. Lyons, J. W. Lyding, and J. R. Tucker, Phys. Rev. B **37**, 10055 (1988).
[4] R. E. Thorne, W. G. Lyons, J. W. Lyding, J. R. Tucker, and J. Bardeen, Phys. Rev. B **35**, 6348 (1987).
[5] R. E. Thorne, W. G. Lyons, J. W. Lyding, J. R. Tucker, and J. Bardeen, Phys. Rev. B **35**, 6360 (1987).
[6] G. Kriza, G. Quirion, O. Traetteberg, W. Kang, and D. Jerome, Phys. Rev. Lett. **66**, 1922 (1991).
[7] N. Kokubo, R. Besseling, V. M. Vinokur, and P. H. Kes, Phys. Rev. Lett. **88**, 247004 (2002).
[8] A. B. Kolton, D. Domínguez, and N. Grønbech-Jensen, Phys. Rev. Lett. **86**, 4112 (2001).
[9] S. P. Benz, M. S. Rzchowski, M. Tinkham, and C. J. Lobb, Phys. Rev. Lett. **64**, 693 (1990).
[10] L. L. Sohn and M. Octavio, Phys. Rev. B **49**, 9236 (1994).
[11] R. C. Dinsmore III, M. H. Bae, and A. Bezryadin, Appl. Phys. Lett. **93**, 192505 (2008).
[12] M. H. Bae, R. C. Dinsmore III, T. Aref, M. Brenner, and A. Bezryadin, Nano Lett. **9**, 1889 (2009).
[13] M. P. N. Juniper, A. V. Straube, R. Besseling, D. G. A. L. Aarts, and R. P. A. Dullens, Nat. Commun. **6**, 7187 (2015).
[14] S. V. Paronuzzi Ticco, G. Fornasier, N. Manini, G. E. Santoro, E. Tosatti, and A. Vanossi, J. Phys.: Condens. Matter **28**, 134006 (2016).
[15] C. Reichhardt, and C. J. Olson Reichhardt, Phys. Rev. B **95**, 014412 (2017).
[16] O. Braun and Yu. S. Kivshar, *The Frenkel-Kontorova Model* (Springer, Berlin, 2003).
[17] J. Tekić and P. Mali, *The ac Driven Frenkel-Kontorova Model* (University of Novi Sad, Novi Sad, 2015).
[18] R. L. Kautz, Rep. Prog. Phys. **59**, 935 (1996).
[19] L. M. Floría and J. J. Mazo, Adv. Phys. **45**, 505 (1996).
[20] F. Falo, L. M. Floría, P. J. Martínez, and J. J. Mazo, Phys. Rev. B **48**, 7434 (1993).
[21] L. M. Floría and F. Falo, Phys. Rev. Lett. **68**, 2713 (1992).
[22] J. Tekić, O. M. Braun, and B. Hu, Phys. Rev. E **71**, 026104 (2005).
[23] A. Vanossi and O. M. Braun, J. Phys.: Condens. Matter **19**, 305017 (2007).

[24] A. Vanossi, J. Röder, A. R. Bishop and V. Bortolani, Phys. Rev. E **67**, 016605 (2003).
[25] A. Zettl, C. M. Jackson, and G. Grüner, Phys. Rev. B **26**, 5773 (1982).
[26] P. Bak, Phys. Today **39**(12), 38 (1986).
[27] M. H. Jensen, P. Bak, and T. Bohr, Phys. Rev. Lett. **50**, 1637 (1983).
[28] M. H. Jensen, P. Bak, and T. Bohr, Phys. Rev. A **30**, 1960 (1984).
[29] T. Bohr, P. Bak, and M. H. Jensen, Phys. Rev. A **30**, 1970 (1984).
[30] I. Sokolović, P. Mali, J. Odavić, S. Radošević, S. Yu. Medvedeva, A. E. Botha, Yu. M. Shukrinov, and J. Tekić, Phys. Rev. E **96**, 022210 (2017).
[31] A. A. Middleton, Phys. Rev. Lett. **68**, 670 (1992).
[32] A. A. Middleton and D. S. Fisher, Phys. Rev. B **47**, 3530 (1993).
[33] R. L. Kautz and R. Monaco, J. Appl. Phys. **57**, 875 (1985).
[34] Yu. M. Shukrinov, A. E. Botha, S. Yu. Medvedeva, M. R. Kolahchi and A. Irie, Chaos **24**, 033115 (2014).
[35] A. E. Botha, Yu. M. Shukrinov, S. Yu. Medvedeva, and M. R. Kolahchi, J. Supercond. Novel Magn. **28**, 349 (2015).
[36] A. E. Botha, Yu. M. Shukrinov, and M. R. Kolahchi, Nonlinear Dynam. **84**, 1363 (2015).
[37] Yu. M. Shukrinov, M. Hamdipour, M. R. Kolahchi, A. E. Botha, and M. Suzuki, Phys. Lett. A **376**, 3609 (2012).
[38] B. Hu and J. Tekić, Phys. Rev. E **75**, 056608 (2007).
[39] B. Hu and J. Tekić, Appl. Phys. Lett. **90**, 102119 (2007).
[40] B. Hu and J. Tekić, Phys. Rev. E **72**, 056602 (2005).
[41] J. Tekić and B. Hu, Appl. Phys. Lett. **95**, 073502 (2009).
[42] J. Tekić and B. Hu, Phys. Rev. E **81**, 036604 (2010).
[43] J. Odavić, P. Mali, J. Tekić, M. Pantić and M. Pavkov-Hrvojević, Commun. Numer. Sci. Nonlinear Simulat. **47**, 100 (2017).
[44] C. Baesens, Spatially extended systems with monotone dynamics (Continuous Time), in *Dynamics of Coupled Map Lattices and of Related Spatially Extended Systems*, Lecture Notes in Physics, Vol. 671 (Springer, Berlin/Heidelberg, 2005).
[45] C. Baesens and R. S. MacCay, Nonlinearity **17**, 567 (2004).
[46] J. Odavic, P. Mali, and J. Tekić, Phys. Rev. E **91**, 052904 (2015).
[47] Yu. M. Shukrinov, S. Yu. Medvedeva, A. E. Botha, M. R. Kolahchi, and A. Irie, Phys. Rev. B **88**, 214515 (2013).
[48] M. Nashaat, A. E. Botha, and Yu. M. Shukrinov, Phys. Rev. B **97**, 224514 (2018).
[49] M. J. Renné and D. Polder, Rev. Phys. Appl. **9**, 25 (1974).
[50] J. R. Waldram and P. H. Wu, J. Low Temp. Phys. **47**, 363 (1982).
[51] O. M. Braun, T. Dauxois, M. V. Paliy, and M. Peyrard, Phys. Rev. Lett. **78**, 1295 (1997).
[52] O. M. Braun, A. R. Bishop, and J. Röder, Phys. Rev. Lett. **79**, 3692 (1997).
[53] O. M. Braun, T. Dauxois, M. V. Paliy, and M. Peyrard, Phys. Rev. E **55**, 3598 (1997).
[54] M. V. Paliy, O. M. Braun, T. Dauxois, and B. Hu, Phys. Rev. E **56**, 4025 (1997).
[55] L. F. Rokhinson, X. Liu, and J. K. Furdyna, Nat. Phys. **8**, 795 (2012).